Virtual Characterization of the Pore Structure of Nonwoven

Andreas Wiegmann and Jürgen Becker
Fraunhofer Institut für Techno- und Wirtschaftsmathematik,
Kaiserslautern, Germany

Abstract

Nonwoven may be digitized by two methods: as images taken from real media, or as generated computer representations obtained from average properties of real media (porosity, fiber diameters, and fiber orientation). Given an accurate correlation between reality and the computer representation of nonwoven, the use of generated media can accelerate the search for potential improvements. We discuss the computer simulation of mercury intrusion porosimetry by the pore morphology method, and present some examples. Through the pore morphology method, it is possible to establish links between production parameters like grammage and fiber diameters, and the porosimetry measurements. Real media experiments would require more effort, cost and time. Automation of the procedure, from fiber generation to property computation, allows deriving analytic formulas for pore size measures depending on production parameters.

Keywords: nonwoven model, mercury intrusion porosimetry simulation, analytic formula for mean pore sizes.

Introduction

Computer simulations represent a potential revolution for the industrial nonwoven development process. Manmade fibers are uniform and designable. Nonwoven media parameters, like porosity, fiber thickness distribution, fiber orientation and porosity gradients are largely controlled by the experienced nonwoven designer and manufacturer. Still, the cost of assessing new parameter sets is usually high. Nonwoven fabrication at laboratory scale is often in conflict with nonwoven manufacture at production scale, and halting the production lines during parameter studies is especially expensive. Computer simulations can significantly reduce the number of trial runs for the development new material prototypes. Understanding of production processes and nonwoven functionality may be improved using computer simulations. They may reveal new trends or improvements that would be costly to discover using traditional methods. Consequently, much work has been devoted to the study and imaging of nonwoven, and to building nonwoven models [1, 2, 3, 4, 5, 6, 7, 8]. As a result, the pore size distribution of nonwoven can be analyzed, predicted and optimized [9, 10] based on analytical methods [11], indirect pore size measurements [12] or analysis of three-dimensional images of nonwoven.

Obtaining the nonwoven structure: Imaging vs. Generation

Starting point of our pore structure characterization method is the construction of a three dimensional microscopic model of the nonwoven. Such a model can be obtained either from an image of the nonwoven (DVI, tomography, etc.), or by virtually generating a three dimensional model. While real images might be used when comparing measurement and simulation, computer generated models are necessary when designing new materials. In addition to the cost of acquiring the three-dimensional image, the final influence of image processing procedures used to obtain a binary image from a real nonwoven must be considered. Due to this influence, we apply the pore structure characterization to virtual nonwoven, albeit the method equally applies to images of real media. The virtual reconstruction of the nonwoven uses as input statistical material parameters such as porosity and mean fiber thickness, and applies methods from statistical geometry to generate a model (see also [1,2,13]). Nevertheless, if the generated sample represents a large enough part of the porous media, the results are representative.
To demonstrate the numerical methods presented in the following we generated a nonwoven fiber mat with a size of 512 µm x 512 µm x 128 µm, and an overall porosity of 82%. The resolution is 1 µm per voxel. The fibers have a circular cross section, a diameter of 7 µm, and are oriented along the x-y plane. Figure 1 shows a visualization of the created nonwoven structure.

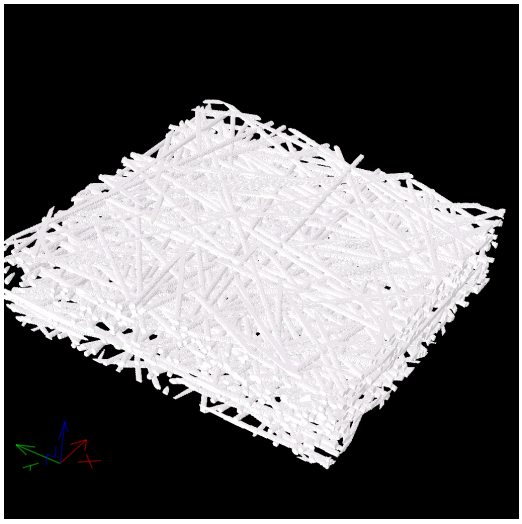

Figure 1: 3d visualization of a generated nonwoven (from [10], using [13]).

Mercury intrusion porosimetry: Measurement vs. Simulation

As mercury is non-wetting to most materials, intrusion of mercury into pores only occurs when pressure is applied on the mercury. In the experimental setup [12], the pressure on the mercury is subsequently raised, and the volume of the intruding mercury (which equals the volume of the intruded pores) is measured. The pressure p is related to the pore radius r via

the Young-Laplace equation $$p = \frac{2\gamma}{r}\cos\vartheta, \qquad (1)$$

where γ is the surface tension and ϑ the contact angle of mercury. Thus, a size distribution of pores is determined. This method cannot measure the volume of closed pores. Furthermore, large pores hidden behind smaller bottlenecks are not filled with mercury until the pressure is high

enough for the mercury to pass the bottleneck. Thus, these pores are measured with the size of the bottleneck. In nonwoven, these limitations generally do not play a role.
To mimic this experimental setup in the simulation, only pores connected to the mercury reservoir must be taken into account. This is algorithmically achieved by first eroding the pore space by r, and then, in a second step, discarding the parts not connected to the reservoir. In the third step, the remaining pore space is dilated by r again. The resulting pore volume is exactly that part of the pore volume reachable by a sphere of radius r flowing in from the reservoir [Hil01].
Figure 3 illustrates this approach by showing the results of the method in a two dimensional example. Here, it was assumed that the mercury might intrude the nonwoven structure from the top, and from the bottom. A comparison of the results shown in Figure 2 and Figure 3 shows that the cumulative volume fraction of the pores with radius $r \geq 20$ or $r \geq 16$ is much lower when measured with mercury intrusion porosimetry.
Simulations performed on the sample shown in Figure 1 are illustrated in Figure 2.

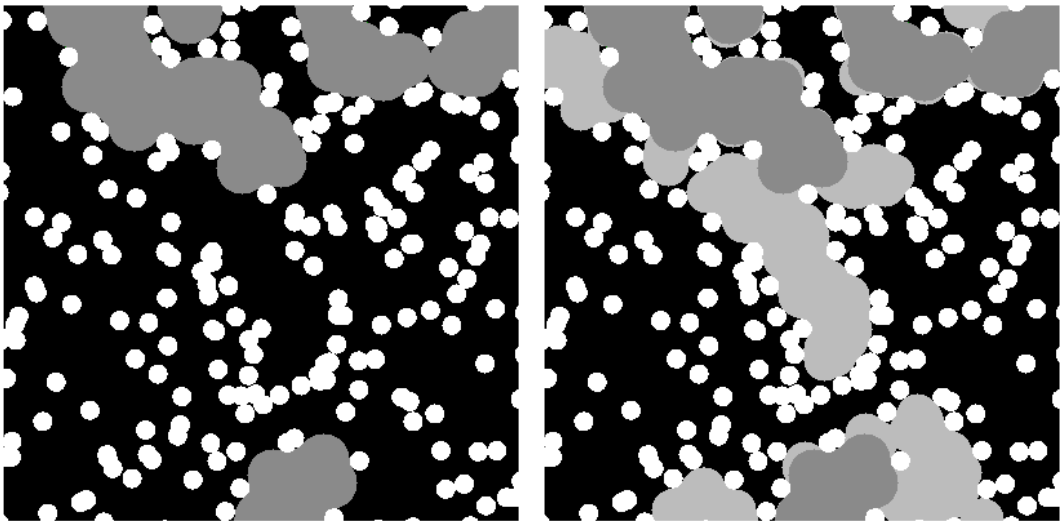

Figure 2: Two dimensional view illustrating the method of a mercury intrusion porosimetry simulation. Fibers are white, and grey areas indicate pores of radius $r \geq 20$ and $r \geq 16$, respectively. All marked pores are always connected to one of the mercury reservoirs on top or bottom of the sample by a wide enough path. (from [10], using [13]).

Besides mercury intrusion porosimetry, [10] also considers geometrical pore size distributions and liquid extrusion porosimetry. The differences between the different methods are significant, just as in real measurements, and illustrated in Figure 3. The studies in the next sections could be equally well performed on these other measures of pore sizes if needed for agreement with real measurements.

Derivation of analytic formulas for grammage and fiber diameter variations

New nonwoven applications in other areas, such as filtration, require a media designed to particular pore size specifications [11], leading to an increased interest in analytic formulas for the pore size distributions in nonwoven. We derive these formulas, in an exemplary way, using the automated nonwoven generation and the pore size evaluation capabilities of [13], combined with some conventional data analysis that is more common in experimental setups.

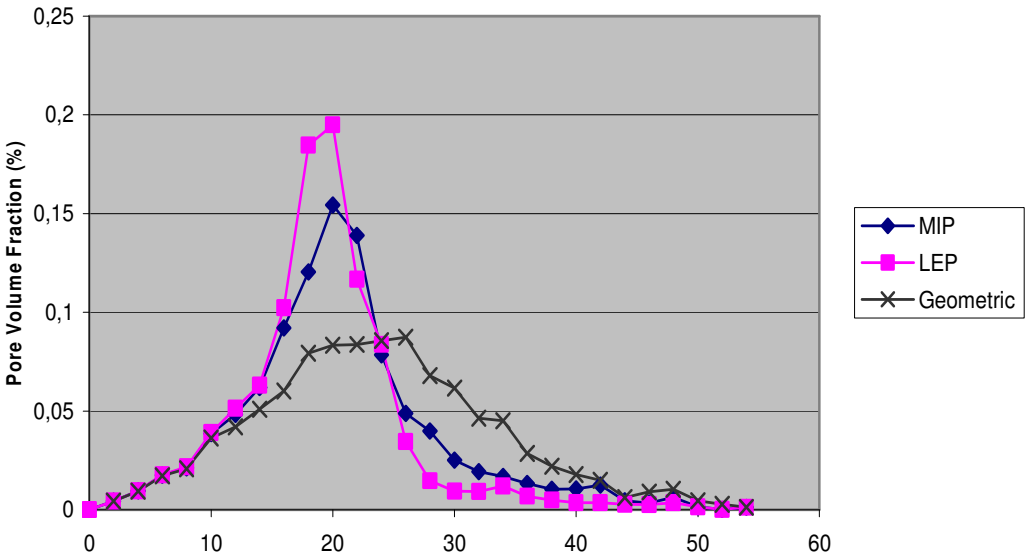

Figure 3: Pore size distribution of the sample shown in Figure 1. The diagram shows the calculated geometric pore size distribution and the results of the simulated mercury intrusion porosimetry (MIP) and the simulated liquid extrusion porosimetry (LEP) (from [10]).

We consider that the D10, D50 and D90, i.e. the 3 pore sizes, are such that 10, 50, or 90 percent of the pores are smaller than the given size. Two single variable computer experiments are carried out. First, we study the dependence of the D10, D50 and D90 on the nonwoven grammage. Second, we assess the dependence of the D10, D50 and D90 on the fiber diameter. All other parameters remain fixed. Table 1 and Table 2 summarize these two inquiries. Of course, when the thickness of the nonwoven is kept fixed, the variation of solid volume fraction is directly proportional to grammage.

Exp. A	case 1	case 2	case 3	case 4	case 5	case 6	case 7
Fiber diameter	28µm	28µm	28µm	28µm	28µm	28µm	28µm
SVF	0.02	0.04	0.06	0.08	0.10	0.12	0.14

Table 1: Experiment **A**: Variation of porosity (1 – Solid Volume Fraction, SVF).

Exp. B	case 1	case 2	case 3	case 4	case 5	case 6	case 7
Fiber diameter	22µm	24µm	26µm	28µm	30µm	32µm	34µm
SVF	0.08	0.08	0.08	0.08	0.08	0.08	0.08

Table 2: Experiment **B**: Variation of fiber diameter at fixed Solid Volume Fraction (SVF).

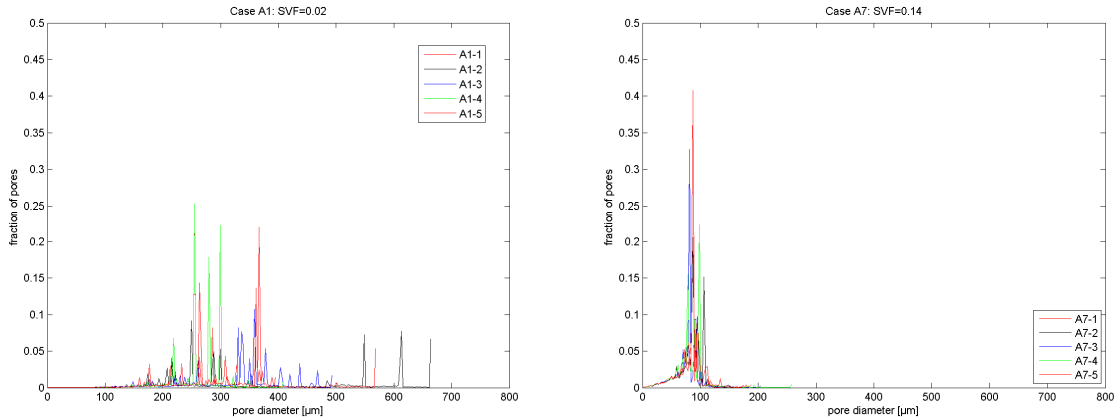

Figure 4: Pore sizes distributions for five realizations of SVF 0.02 (left) and for five realizations of SVF 0.14 (right), Experiment **A**. The variation is much higher for smaller SVF.

The 14 cases represent 13 different nonwoven designs because A4 and B4 are identical. For each of the designs, 5 realizations of 840µm by 840µm by 840µm at a resolution of 2.8µm per voxel were created. The sample size was thus 300^3 voxels, which must be regarded as a minimum size when considering the variations in the pore size distributions visible in Figure 4. This figure illustrates the computed pore sizes over the 5 samples for SVF 0.02 and SVF 0.14, respectively.

The parameter sets were generated by exporting one structure from **GeoDict** [13], and manually copying and modifying the parameters for the other cases in a macro file. Five virtual probes with the same statistics were created using identical parameters, but different detailed fibers locations due to a different initialization of the random number generator. The automated generation and pore size distribution analysis of these 65 large data sets by virtual mercury intrusion porosimetry took up 36 hours on a desktop personal computer running the **GeoDict** [13] modules **FiberGeo** and **PoroDict**.

Figure 5 shows the pore size distribution for experiment **A** as averages over the 5 realizations. As expected, a lower solid volume fraction (i.e., higher porosity) leads to larger pores. It is worth mentioning that for lower solid volume fraction, the variation of the curves increases.

Figure 6 shows the pore size distribution for experiment **B** as averages over the 5 realizations. As expected, larger fiber diameters lead to larger pores. Since the SVF, or grammage, is fixed in this case, the pore sizes vary far less than in the case of experiment A, where the grammage varies. In order to arrive at quantities for which an analytical formula may be derived, we next consider the D10, D50 and D90 for the two experiments. Thus, we arrive at a functional relation relating the grammage to mean pore size, and at a relation relating fiber diameter to mean pore size.

The curves shown in Figure 7 and Figure 8, suggest a specific dependence of mean pore diameters on the respective variable (grammage and fiber diameter).

In Figure 7, the pore diameters are shown as function of grammage. Clearly, the pore diameter tends to infinity for vanishing grammage, and to zero for maximum grammage (zero porosity or SVF=1). From this, the ansatz function

$$f = \alpha \frac{1-s}{s^{\beta}} \quad (2)$$

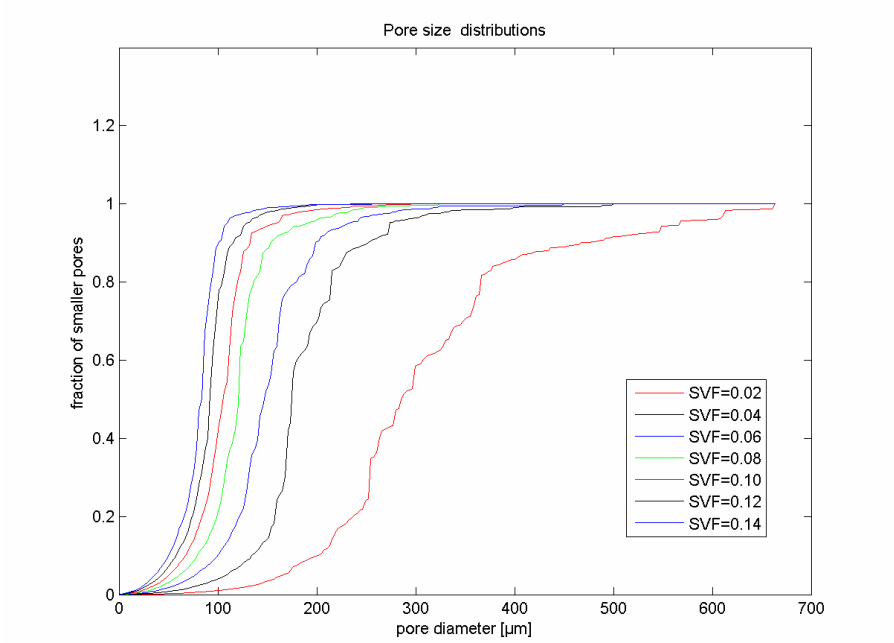

Figure 5: Pore size distributions for various SVFs, Experiment **A**.

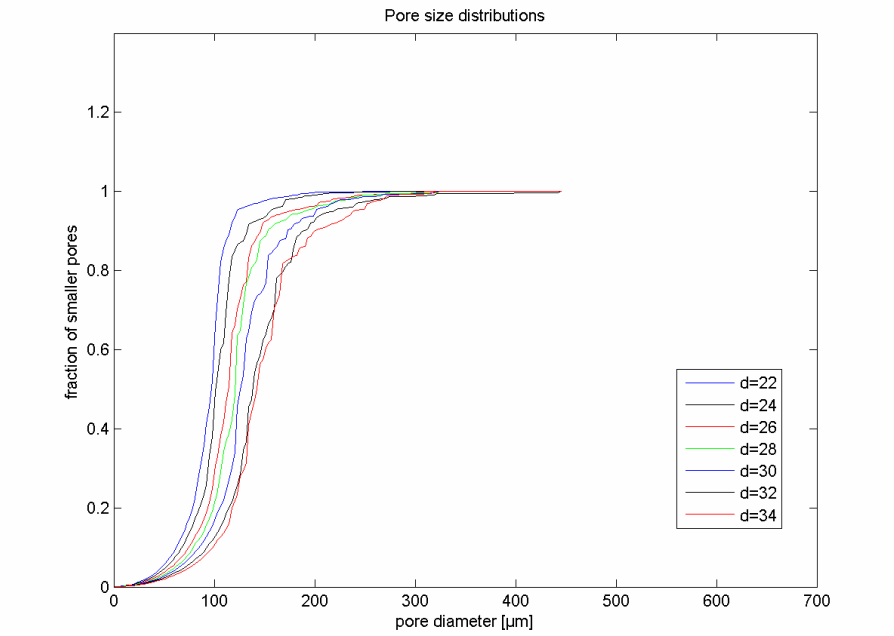

Figure 6: Pore size distributions for various fiber diameters, Experiment **B**.

with the two parameters α and β is guessed, where s is the SVF. The values found by regression (after taking the logarithm) are given in Figure 6. The fit is excellent, and the values suggest that β might not even depend on the SVF.

In Figure 8, pore diameters are shown as function of fiber diameter. The pore diameter should tend to zero as the diameter goes to zero. From the shape of the curves, the ansatz function

$$f = \lambda d \qquad (3)$$

with the parameter λ is guessed, where d is the fiber diameter. The values found by linear regression are given in Figure 8. Again, the fit is excellent.

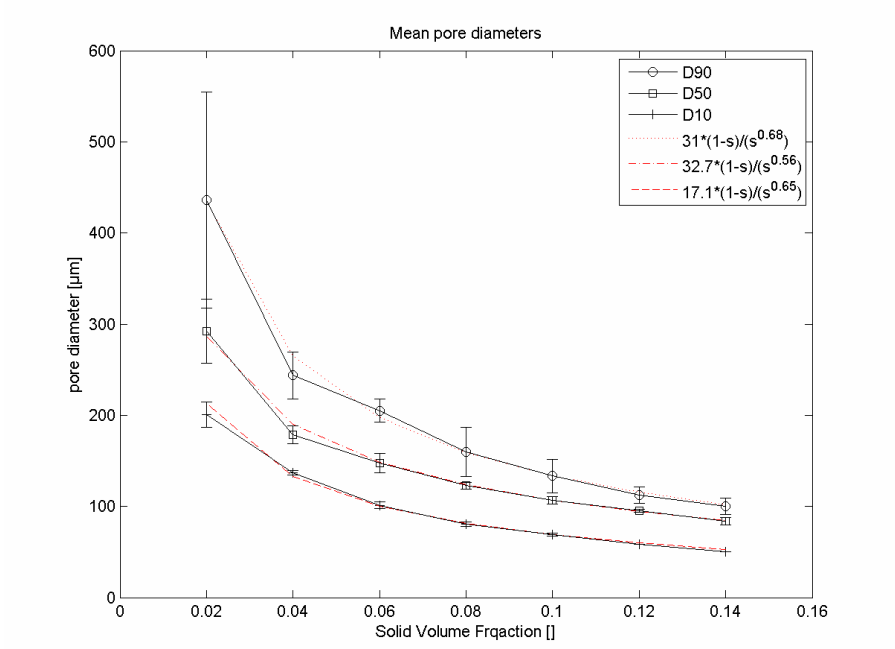

Figure 7. Variation of D10, D50 and D90 depending on grammage.

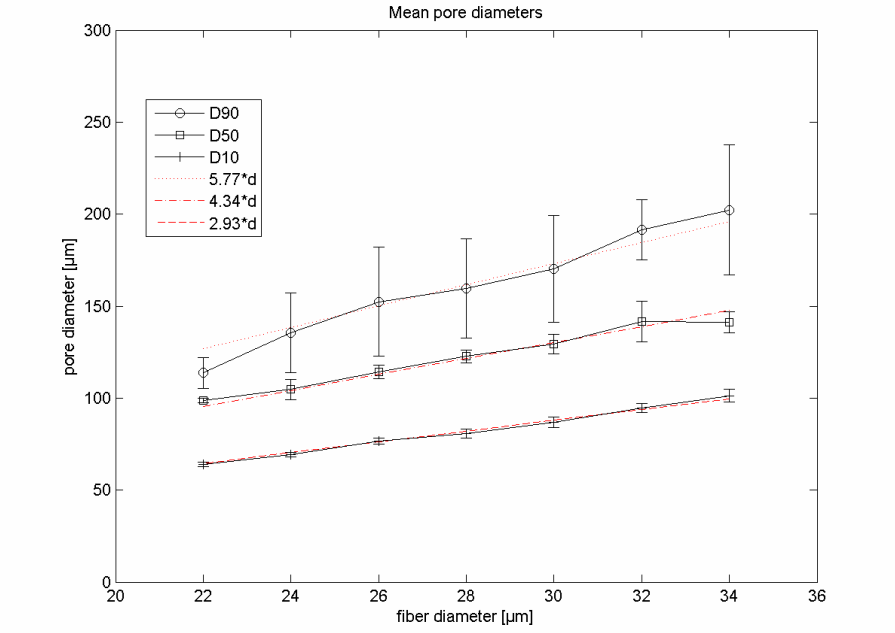

Figure 8. Variation of D10, D50 and D90 depending on fiber diameter.

Conclusions

The described methodology of modeling nonwoven media, together with the simulation of pore size distributions, provides easy insights into the behavior of complex filter media. The automation of the procedure considerably eases the effort of studying a variety of parameters. This includes multi-variable studies, such as combining fiber diameters and grammage into a single analytic formula. In the future, such studies should pursue the analysis of three-dimensional images of real media and not exclusively the study of computer models. The results of the analysis should be compared to measurements of mercury intrusion porosimetry. Also liquid extrusion porosimetry could also be considered in the future. Complete simulations can be carried out on desktop PCs, and can be tested by interested parties by downloading the Software for evaluation purposes from http://www.geodict.com. The examples in this document can be obtained from the authors.

References

[1] J. Ohser u. F. Mücklich, *Statistical Analysis of Microstructures in Materials Science*, John Wiley & Sons (2000).

[2] K. Schladitz, S. Peters, D. Reinel-Bitzer, A. Wiegmann, J. Ohser, *Design of acoustic trim based on geometric modeling and flow simulation for nonwoven*, Comp. Mat. Sci. 38, 56-66 (2006).

[3] H. Yang and W.B.Lindquist. *A Geometric Analysis on 3D Fiber Networks from High Resolution Images.* International Nonwovens Technical Conference, Dallas, 2000.

[4] B. Pourdeyhimi, *Assessing Fiber Orientation in Nonwoven Fabrics*, INDA Journal of Nonwovens Research, 5, (3), 29-36, (1993).

[5] B. Pourdeyhimi and H. S. Kim, *Measurement of Fiber Orientation in Nonwovens: Hough Transform*, Textile Research Journal, 72 (9), 803-809 (2002)

[6] X. Thibault and J.F. Bloch, *Structural Analysis by X-ray Microtomography of Strained Nonwoven Papermaker Felt*. Textile Research Journal, 72 (6), 480-485, 2002.

[7] T. Gilmore, H. Davis, Z. Mi. *Tomographic Approaches to Nonwovens Structure Definition*. National Textile Center Annual Report. September 2004.

[8] R.L. Kerschmann, *DVI: Digital Volumetric imaging*. MicroScienceGroup, www.microsciencegroup.com.

[9] V. Schulz, J. Becker, A. Wiegmann, P. Mukherjee and C.-Y. Wang. *Modelling of Two-phase Behaviour in the Gas Diffusion Medium of Polymer Electrolyte Fuel cells via Full Morphology Approach*, J. Electrochem. Soc., 154 (4), 2007.

[10] J. Becker, A. Wiegmann and V. Schulz, *Design of fibrous filter media based on the simulation of pore size measures*, Filtech Europa, Wiesbaden, February 2007.

[11] G.E. Simmonds, J.D. Bomberger and M.A. Bryner, *Designing nonwovens to Meet Pore Size Specifications,* Journal of Engeineered Fibers and Fabrics, 2 (1) 2007.

[12] A. Jena and K. Gupta. *Characterization of pore structure of filtration media, Fluid Particle Separation Journal,* Vol. 4, No.3, pp. 227-241, 2002.

[13] A. Wiegmann, ***GeoDict*** *Software*, www.geodict.com, ©2001-2007.